Chromatographic Analyses, Virtual Screening and Pharmacokinetics of Yellow Malaysian Rambutan (Nephelium lappaceum L.) Fruit Epicarp Extracts Reveal Potential Antibacterial Compounds

Ali Asghar
Sunway University
Yong Chiang Tan
Sunway University
Mohammad Zahoor
University of Malakand
Syafiq Asnawi
Monash University Malaysia
Yoon-Yen Yow
Sunway University
Ezzat Khan
University of Bahrain
Chandrajit Lahiri (chandrajitl@sunway.edu.my)
Sunway University

Research Article

Keywords: Antimicrobial Resistance, Nephelium lappaceum, Bioactive Compounds, Virtual Screening, DnaK

Posted Date: December 23rd, 2020

DOI: https://doi.org/10.21203/rs.3.rs-125241/v1

Version of Record: A version of this preprint was published at Scientific Reports on July 5th, 2021. See the published version at https://doi.org/10.1038/s41598-021-92622-0.

Abstract

The emergence and spread of antimicrobial resistance have been of serious concern on human health and the management of bacterial infectious diseases. Effective treatment of these diseases requires the development of novel therapeutics, preferably free of side effects. In this regard, natural products are frequently conceived to be potential alternative sources for novel antibacterial compounds. Herein, we have evaluated the antibacterial activity of the epicarp extracts of the Malaysian cultivar of yellow rambutan fruit (*Nephelium lappaceum L.*) against six pathogens namely, *Bacillus subtilis*, methicillin-resistant *Staphylococcus aureus* (MRSA), *Streptococcus pyogenes, Pseudomonas aeruginosa, Klebsiella pneumoniae* and *Salmonella enterica*. Among a series of solvent extracts, fractions of ethyl acetate and acetone have revealed significant activity towards all tested strains. Chemical profiling of these fractions, via HPLC, LC-MS and GC-MS, has generated a library of potential bioactive compounds. Downstream virtual screening, pharmacological prediction, and receptor-ligand molecular dynamics simulation have eventually unveiled novel potential antibacterial compounds, which can be extracted for medicinal use. To this end, we report novel mechanistic aspects of these compounds in competitively inhibiting the ATP-binding domain of the DnaK chaperone of *P. aeruginosa* and MRSA. Our work takes a step forward to discover antimicrobials capable of perforating the barrier of resistance posed by both the gram positives and the negatives.

Introduction

Antimicrobial resistance (AMR) has been projected as one of the serious global concerns with issues in the management of infectious diseases caused by Multidrug Resistant (MDR) bacterial pathogens[1]. These pathogens have been reported to cause 700,000 deaths each year which is estimated to cross over 10 million by 2050[2]. Such alarming rise can be attributed mostly to the prevalent misappropriation of antibiotics in human healthcare systems[3] delineated by the overuse and poor appropriate prescriptions coupled with the lack of new drug development, which have reduced the efficiency of antibiotics as the resistant strains rapidly increases[4]. This necessitates the urgency for unearthing alternate natural therapeutics focused on natural products to be exploited as repertoires of natural bioactive compounds, preferably devoid of side effects and hence, potential for future drug development.

Natural products, frequently discovered with potent antimicrobial potential, have been used as alternatives with the hope of eliminating the use of synthetic antibiotics, since a long time[5]. Besides serving a widespread range of secondary plant metabolites, for instance, alkaloids, tannins, flavonoids and phenolic compounds, with remarkable antimicrobial effects[6], many plant products have been reported for their antimicrobial potentials, namely, citrus peel[7], grape seed[8], cranberry pomace[9], pomegranate peel[10] and passion fruit seed[11]. In this regard, the fruit rambutan (*Nephelium lappaceum L.*) has gained attention due to its vast range of bioactive constituents including, but not limited to, vitamin C, vitamin E, carotenes, xanthophylls, tannins and phenolic compounds like, geraniin, ellagic acid, quercetin, corilagin and rutin[12].

While the broad range of biological activities of rambutan include anticancer, antiproliferative and anti hypercholesterolemic properties[13,14], few researchers have even reported its *in vitro* antibacterial activities. For instance, Malini & Maheshkumar[15] have disclosed significant antibacterial activity of rambutan fruit sap extracts towards *Pseudomonas aeruginosa* while Bhat and Al-daihan[16] revealed antibacterial activities of its seeds extracts against *Staphylococcus aureus, Streptococcus pyogenes, Bacillus subtilis, Escherichia coli* and *P. aeruginosa.* Moreover, antibacterial potential of rambutan peel extracts have also been reported against *Vibrio cholerae, Enterococcus faecalis, S. aureus* and *Staphylococcus epidermidis*[17]. Furthermore, Sekar *et al.*[18] comparatively evaluated the antibacterial potency of red and yellow rambutan fruit peels against *S. aureus and S. pyogenes*, to reveal better efficacy of the latter extracts against the tested pathogens.

In this study, we have delineated a stepwise approach of determining the efficacy of the crude extracts of the epicarp of yellow Malaysian rambutan against clinically important MDR bacterial pathogens e.g. *B. subtilis*, methicillin-resistant *S. aureus* (MRSA), *S. pyogenes, P. aeruginosa, K. pneumoniae* and *S. enterica*. Further chemical profiling of the extracts through HPLC, LC-MS and GC-MS revealed their potential chemical determinants which were screened virtually to pharmacologically unveil novel bioactive compounds through molecular dynamics simulation. To this end, a competitive inhibition of the ATP-binding domain of the DnaK chaperone of *P. aeruginosa* and MRSA, by our shortlisted compounds, portrayed novel antibacterial mechanism, representative of targeting both the gram-positive and the -negative pathogens.

Results

Variable antibacterial activity of crude extracts by disc diffusion

A preliminary screening for the antibacterial activities of the yellow-variety Malaysian Rambutan epicarp crude extracts was assessed through disc diffusion assay. Only freshly prepared solutions were used for all the tested pathogens (TP) for the crude extracts. Throughout such trials, the solvent control (SC), DMSO, showing no inhibtion zone, did not exercise antibacterial activity against the TP. Moreover, none of the sequential extracts exhibited activity against the TP (Table 1, **Fig. S1**), while in case of direct extracts, the picture was quite different. Extracts of ethyl acetate (EA) displayed visible activity against MRSA, *B. subtilis* and *S. enterica* but did not show activity against the rest of the TP (RTP). Again, acetone (AC) extracts exhibited markedly prominent activity against *B. subtilis* along with visible acitivty against *S. pyogenes* and *P. aeruginosa*, which was not observed among the RTP (Table 1, **Fig. S2**).

Table 1
Antibacterial activity of the sequential and direct crude extracts of *N. lappaceum* by disc diffusion

	Visible inhibition produced by extracts							
Extracts	B. subtilis	**MRSA**	S. pyogenes	P. aeruginosa	K. pneumonia	S. enterica	**S.C**	**P.C**
EA(S)	-	-	-	-	-	-	-	++
AC(S)	-	-	-	-	-	-	-	++
EA(D)	+	+	-	-	-	+	-	++
AC(D)	++	-	+	+	-	-	-	++

+: Visible; ++: Prominent; -: No activity; EA: Ethyl acetate; AC: Acetone S: Sequentila; D: Direct; S.C: Solvent control (DMSO); P.C: Positive control (Gentamicin 10 µg)

Qualitative antibacterial screening of crude extracts via Broth dilution

Broth dilution method was used for evaluating the antibacterial potential of yellow fruit epicarp crude extracts and calculating the viability percentage of every TP (Table 2). This in turn illustrated the percentages of antibacterial potential of EA and AC fractions from the sequential & direct extracts, against the TP, at concentration of 250 µg/mL. For the sequential extracts, the fraction from AC exhibited the highest percentage (90) of antibacterial activity against *P. aeruginosa* followed by 71% against MRSA while that from EA exhibited 59% effect against *S. pyogenes*. No significant results were observed either against the RTP (Fig. S3 a-f) or for the remaining solvent extracts namely, chloroform (CF), ethanol (ET), methanol (MT) and aqueous (water, WT) extracts against all TP (**Table S2**). In the case of direct extracts with the six solvents used, fractions of EA exhibited inhibition of 80% against *B. subtilis* along with 60, 62, 73 and 72% for MRSA, *P. aeruginosa, S. enterica* and *K. pneumonia*, respectively, without any positive results against *S. pyogenes*. Notably, all tested pathogens were inhibited by AC fractions and the percentage of antibacterial effects were 75, 90, 70, 70, 60 and 75, respectively for MRSA, *B. subtilis, S. pyogenes*, *P. aeruginosa, S. enterica* and *K. pneumonia* (**Fig. S3 g-l**).

Table 2
Screening of antibacterial effect of sequential and direct extracts by broth dilution method

% Viability of all tested pathogen						
Microorganisms	**EA(S)**	**EA(D)**	**AC(S)**	**AC(D)**	**S.C**	**P.C**
B. subtilis	-	20	-	10	98	0
MRSA	-	40	29	25	98	0
S. pyogenes	41	-	-	30	98	0
P. aeruginosa	-	38	10	30	98	0
K. pneumonia	-	28	-	25	98	0
S. enterica	-	27	-	40	98	0

EA(S): ethyl acetate sequential; AC(S): acetone sequential; EA(D): ethyl acetate direct; AC(D): acetone direct; S.C: solvent control: DMSO (< 1%), P.C: positive control (Gentamicin 10 µg); -: Low activity (less than 50%).

The results of EA and AC fractions portrayed notable antibacterial efficiency and were, thus, processed for identification of bioactive compounds via HPLC, LC-MS and GC-MS analyses.

Revelation of antioxidants from crude extracts using HPLC-UV

For a preliminary identification of the basic antioxidants present in the Malaysian yellow-rambutan epicarp extracts, HPLC-UV was conducted. All compounds with known antioxidant capacities were identified in comparison with standard phenolic compounds. The identified compounds and their quantification, along with their specific peak position and retention time (Rt) in chromatogram, are shown in Table 3 and **Fig. S4**. Only three compounds were identified in the EA extract namely, malic acid, vitamin C and chlorogenic acid along with three more in the AC extract. These are epigallocatechin gallate, catechin hydrate and quercetin.

Table 3
Identified compounds in *N. lappaceum* ethyl acetate and acetone sequential fractions using HPLC-UV.

Sample Extract	RT (min)	Identified compounds	Peak Area
EA (S)	12.9	Malic acid	40.441
	4.8	Vitamin C	1717.201
	6.2	Chlorogenic acid	190.156
AC (S)	2.9	Malic acid	4.938
	4.8	Vitamin C	1226.316
	6.2	Chlorogenic acid	134.587
	8.8	Epigallocatechin gallate	205.717
	10.7	Quercetin	85.112
	20.7	Catechin Hydrate	44.169

EA (S): Ethyl acetate sequential fraction; AC (S): Acetone sequential fraction

Exploration of other chemical determinants through Liquid Chromatography–Mass Spectrometry (LC-MS) Analysis

For a fast, mass-directed exploration of the compounds possibly present in the rambutan epicarp, its EA and AC sequential crude extracts were subjected to LC-MS analysis (**Fig. S5 and Fig. S6**) which revealed the presence of 54 and 44 compounds, respectively (**Table S3 & S4**). They were matched with the identity of known molecules on the Metlin database, keeping a threshold Molecular Formula Generator (MFG) scores above 86% along with a ± 2% difference. The compounds above the mentioned cut-off were further explored for their biological activities and carried forward for virtual screening. Notably, 31 compounds from both sets of EA and AC extracts have not been reported till date with any antibacterial activities (**Table S3 & S4**).

Identification of volatile constituents by Gas chromatography–mass spectrometry (GC-MS)

To identify any volatile organic compounds, present in the EA and AC extracts of Malaysian yellow-variety *N. lappaceum* epicarp, they were exposed to GC-MS analysis (**Fig. S7 a-d**). Most of the compounds from EA and AC fractions, extracted directly, have been reported with antibacterial activities (Table 4). On the contrary, the compounds of these fractions from sequential extraction have not been reported for any such activity. The chromatogram of these compounds showed mentionable area % scores (above 0.5%) for 3-Methyl-1,2-diazirine (compound 1) and Card-20(22)-enolide, 3-[(6-deoxy-3,4-O-methylenehexopyranos-2-ulos-l-yl) oxy]-5,11/14-trihydroxy-12 -oxo-, (3-beta, 5-alpha, 11-alpha) (compound 2) in the EA extract while, the AC extract showed the presence of Silane, [[(3alpha,5beta,20S)-

pregn-11-ene-3,11,17,20-tetrayl] tetrakis(oxy)] tetrakis [trimethyl] and 2,2-Bis[4-[(4,6-dichloro-1,3,5-triazin-2-yl) oxy] phenyl]-1,1,1,3,3,3-hexafluoropropane (Table 4). Of these, compound 2 is known as Eplerenone **(Fig. 1)** and was found to be an important one in the upcoming analyses.

Table 4
Compounds existing in *N. lappaceum* ethyl acetate and acetone (sequential & direct) extract identified by GC-MS analysis

No	Extracts	Identified compounds	Molecular Formula	R.T. (Min)	Area %	Antibacterial activity report
1	**EA(S)**	3-Methyl-1,2-diazirine	$C_2H_4N_2$	3.02	0.776	Not reported
2		Card-20(22)-enolide, 3-[(6-deoxy-3,4-O-methylenehexopyranos-2-ulos-l-yl) oxy]-5,11/14-trihydroxy-12 -oxo-, (3-beta.,5-alpha., 11-alpha.)	$C_{30}H_{40}O_{11}$	3.00	3.073	Not reported
3	**AC(S)**	Silane, [[(3alpha,5beta,20S)-pregn-11-ene-3,11,17,20-tetrayl] tetrakis(oxy)] tetrakis [trimethyl]	$C_{33}H_{66}O_4Si_4$	41.85	5.257	Not reported
4		2,2-Bis[4-[(4,6-dichloro-1,3,5-triazin-2-yl) oxy] phenyl]-1,1,1,3,3,3-hexafluoropropane	$C_{21}H_8Cl_4F_6N_6O_2$	3.00	4.241	Not reported
1	**EA(D)**	Phenol, 2,4-bis(1,1-dimethylethyl)	$C_{14}H_{22}O$	10.74	38.698	19
2		Curlone	$C_{15}H_{22}O$	14.44	4.233	20
3		Ar-tumerone	$C_{15}H_{20}O$	18.65	0.857	21
4		Stigmasterol	$C_{29}H_{48}O$	17.87	1.66	22
5		n-Hexadecanoic acid	$C_{16}H_{32}O_2$	48.78	3.2	23
6		3,7,11-Tridecatrienenitrile, 4,8,12-trimethyl	$C_{16}H_{25}N$	23.94	2.567	Not reported
7		2-Methoxy-1,3-dioxolane	$C_4H_8O_3$	39.4	0.563	Not reported
8		5H-Cyclopropa (3,4) benz(1,2-e) azulen-5-one, 1,1a-à,1b-á,4,4a,7a-à,7b,8,9,9a-decahydro-7b-à,9-á,9a-à-trihydroxy-3-hydroxymethyl-1,1,6,8-à-tetramethyl-4a-methoxy-, 9,9a-didecanoate	$C_{41}H_{66}O_8$	58.69	2.34	Not reported

EA(S): Ethyl acetate sequential; AC(S): Acetone Sequential; EA(D): Ethyl acetate direct; AC(D): Acetone direct

No	Extracts	Identified compounds	Molecular Formula	R.T. (Min)	Area %	Antibacterial activity report
1	**AC(D)**	Phenol, 2-methoxy-3-(2-propenyl)	$C_{10}H_{12}O_2$	10.73	0.678	Not reported
2		Phenol, 2,4-bis(1,1-dimethylethyl)	$C_{14}H_{22}O$	14.44	0.912	19
3		Alpha-Tocopherol	$C_{31}H_{52}O_3$	44.65	1.612	24
4		Curlone	$C_{15}H_{22}O$	18.65	1.156	20
5		1,3-Dioxolane, 2-pentadecyl	$C_{21}H_{40}O_4$	57.36	3.06	Not reported
6		Ar-tumerone	$C_{15}H_{20}O$	17.87	4.081	21

EA(S): Ethyl acetate sequential; AC(S): Acetone Sequential; EA(D): Ethyl acetate direct; AC(D): Acetone direct

Short listing of antibacterial compounds via virtual screening and pharmacokinetics

Ensuing virtual screening of 91 chemical compounds obtained through the chromatographic analyses, 41 of them, having binding energy less than − 7 kcal/mol, were considered as good binders (**Table S9**; **Fig. 1, 2A**). Among these, potential drug candidates were chosen based on the predicted pharmacokinetic properties. For example, good gastrointestinal (GI) absorption, bad BBB permeability, and non-P-glycoprotein (PGP) substrates were preferred for absorption properties. For metabolism, non-cytochrome P450 inhibitors were preferred. Violations on drug-likeness rules were, of course, not favored. To cater to the need, five rules have been considered, namely, the Lipinski, Ghose, Veber, Egan, and Muegge rules[25–29]. Lastly, higher bioavailability scores were preferred. The Abbot Bioavailability Score utilized herein was to predict chances of drug bioavailability to be more than 10% upon oral intake[30].

Among the virtually screened compounds, catechin (C), eplerenone (E) and oritin-4-beta-ol (O) stood out to be good binders with their average binding energies being − 8.205, -7.980 and − 7.190 kcal/mol, respectively for *S. aureus* (*Sa*) and *P. aeruginosa* (*Pa*) DnaK proteins. C, E, O also exhibited good predicted pharmacological properties except that C is a PGP substrate **(Fig. 1, Table S9**). The binding conformations of C (**Fig. 2B**), E (**Fig. 2C**), and O (**Fig. 2D**) to both DnaK proteins of *Sa* (SaD) and *Pa* (PaD) showed potential structural competitive inhibition of ATP binding at the docking pocket. Moreover, rich electrostatic interactions (**Fig. 2E**) were observed in C and O, but not in E, having only one intermolecular hydrogen bond.

Validation of inhibitory effects of selected compounds by Molecular Dynamics Simulation

Molecular Dynamics (MD) simulations for 10 nanoseconds were carried out for C, E, and O Ligand-SaD/PaD complexes to observe ligand-receptor interactions. Over the course of MD simulations, the ligands were retained in the docking pocket of respective DnaK receptors, except for C in SaD system (CSaD) of which the ligand seemed to be escaping from the initial binding pocket (**Fig. 3A**; **B**). Moreover, the upper part of the DnaK NBD domain was completely disintegrated in CSaD. Besides, the total number of receptor-ligand intermolecular hydrogen bonds were maintained stably at around 4 and 5 in *P. aeruginosa* DnaK complexed with C (CPaD) and O (OPaD) respectively, and 4 in *S. aureus* DnaK complexed with O (OSaD) (**Fig. 3C**). Moreover, both the E complexes of SaD (ESaD) and PaD (EPaD) have maintained the total number of hydrogen bonds at around 1. However, in CSaD, a sharp decline in the number of intermolecular hydrogen bonds can be observed at 5 ns time point from around 4 to between 0 and 1, which can explain the escape of ligand from its initial docking pocket. Stable active residues have been observed in CPaD (LYS 70, GLU 171, GLU 267), EPaD (ARG 345), and OPaD (THR 11, ASP 194) complexes, as well as in OSaD (GLY 312) complex (**Fig. 3G**).

In all MD simulation systems, the root-mean-square fluctuations of DnaK receptor maintained at around 0.5 nm (5 Å) except for the C-terminal end where the disordered regions were localized (**Fig. 3E**). Besides, the RMSD of C and E maintained at 0.5 nm in PaD receptor, while higher RMSD values of around 0.8 nm have been observed in CSaD and ESaD (**Fig. 3D**). The ligand RMSD were relatively lower in O, compared to others, for which RMSD of 0.4 nm was reported in both SaD and PaD cases. The interaction energies of all systems maintained stably throughout the simulation, except for CSaD complex of which a sharp decrease of Coulomb potential can be observed at around 6 ns time point (**Fig. 3F**). In general, E maintained the lowest total interaction energies, followed by C and O (**Fig. 3H**).

Discussion

Over the years, the commendable development in the field of virtual screening has enabled time- and cost- efficient drug discovery along with repurposing[31]. Herein, we have carried out a scaffolded approach to antimicrobial drug discovery from yellow variety of Malaysian *N. lappaceum L.* fruit epicarp crude extracts. The first upstream set of experimental work comprised the extraction of the plant product, followed by characterization of their antimicrobial property and chromatographic identification of chemical compounds from therein. This was coupled with downstream set of computational analyses comprising virtual screening and pharmacological predictions of extracted chemical compounds against potential drug targets. To this end, molecular dynamic simulation has taken a step forward to uncover new potent bioactive compounds which can target both gram negative and positive bacteria at the same time. Our study delineates a method to uncover potent chemicals which might have contributed in the antibacterial activities of plant products like *Nephelium lappaceum* epicarp, to be further utilized for drug discovery, repurposing, or other *ab initio* synthetic enhancements.

Extraction is the key stage to obtain the diverse bioactive chemical compounds from plant products. These chemical determinants display different solubility with different organic solvents such that a screening with different solvents helps to bring forth the best one for further exploration[32]. Thus, in order

to explore the extraction of biologically active constituents, several organic solvents were utilized in our study. This was initiated with a sequential extraction process of utilizing solvents like chloroform (CF), ethyl acetate (EA), acetone (AC), ethanol (ET), methanol (MT) and water (WT), in order of their increasing polarity. Our study revealed that the yellow variety of Malaysian *N. lappaceum* epicarp crude extracts exhibited varied inhibitory activities against the six tested MDR pathogens, namely, *B. subtilis*, methicillin-resistant *S. aureus* (MRSA), *S. pyogenes, P. aeruginosa, K. pneumoniae* and *S. enterica*. In fact, the EA and AC fractions from the sequential mode remarkably inhibited about all the Gram-positive and Gram-negative tested pathogens (TP) while the remaining solvent fractions responded moderately or poorly, thereby providing a strong clue to proceed for further direct extraction from these solvents. Similar results were obtained from the direct extract fractions of EA and AC showing the least MIC value of 250 µg/mL against the TP. For a double cross-checking, the remaining direct fractions did not inhibit the TP even at the highest concentration of 2000 µg/mL. Despite similar reports to our findings by Mohamed *et al.*[33]; Thitilertdecha *et al.*[34]and Tadtong *et al.*[35], a comprehensive chemical profiling to unearth plausible determinants potential enough against the MDR pathogens is lacking till date.

Based on the prominent antibacterial effects of the EA and AC extracts of *N. lappaceum* fruit epicarp, we perceived that both fractions could harbor important bioactive molecules. Thus, we subjected the sequential extracts of EA and AC fractions to HPLC analysis. The results confirmed the presence of some important phenolic compounds with antioxidant properties namely, malic acid, vitamin C, chlorogenic acid, epigallocatechin gallate, quercetin and catechin hydrate (Table 3**).** Notably, ethyl acetate and acetone have been found to be the competent solvent to extract total flavonoid and phenolic compounds[32]. Nazir *et al.*[36,37], however, reported the aforementioned compounds in various other organic solvent extracts of *Silybum marianum* and *Elaeagnus umbellate*.

To this end, an extensive spectrum of chemical classes was revealed after LC-MS analysis and included, terpenes, alkaloids, polyunsaturated and monounsaturated fatty acids among others, that were present in both the extracts. Among these, only 21 of the 54 compounds (with above 86% MFG scores) of the EA fractions have been reported to possess antibacterial activities **(Table S3).** Interestingly, most of them have been newly reported (within the last five years) including L2[38], L3[39], L6[40], L10[42], L12[43], L16[44], L20[45], L22[47], L26[48], L28[49], L31[50], L46[54], L48[55], L51[56], L53[57] and L54[55]. Others are known for some time, namely, L7[41], L21[46,] L35[51], L37[52] and L45[53.] Similarly, the AC extract fractions contained only 10 from 44 compounds with reported antibacterial activities (Table S4). Of these, except for L24[51] and L35[53], all were reported recently. These included L2[40], L5[58], L10[44], L13[48], L19[50], L36[54], L38[55] and L42[57]. Thus, possibilities exist for those 35 and 26 compounds from EA and AC fractions, respectively, with no matched identity with the library, **(Table S5, S6)**, to be medically important, though, further characterization is required to evaluate their usages.

Further revelation of important biomolecules was authenticated through GC-MS (Table 4) besides the HPLC and LC-MS analyses mentioned above in Tables 3 **& S3-S4**, respectively. Notably, both sequential and direct extracts of EA and AC fractions were analysed through GC-MS. Unlike the LC-MS reported

compounds, however, about 50% of the chemical components, unearthed through GC-MS, are unknown for their antibacterial activity. For instance, in case of sequential extracts, for both the EA and AC fractions, only 4 molecules were detected (with area % scores above 0.5%) without any *a priori* antibacterial activity **(**Table 4**).** Likewise, for the direct extract fractions of EA, only 5 out of 8 compounds detected (with area % scores above 0.5%) were known to possess such activity. These are DGEA1[19], DGEA2[20], DGEA3[21], DGEA4[22] and DGEA5[23]. However, for the AC extract fraction, 4 out of total 6 compounds detected, were reported to possess the antibacterial effect. These are DGAC2[19], DGAC3[24], DGAC4[20] and DGAC6[21].

With a set of 91 compounds obtained through chromatographic analyses, we have conducted a computational analysis for virtual screening through molecular docking to short list a selective set of chemicals via pharmacokinetics consideration (Table S9). Pharmacokinetics is an important criterion when it comes to drug discovery and drug design, especially pertaining to bioavailability and toxicity. Herein, we have considered several parameters for absorption, metabolism, drug-likeness, and bioavailability for selecting the ideal drug for potential pharmacological application in the future. For instance, good GI absorption can allow absorption into bloodstream during oral consumption, while bad blood-brain barrier (BBB) permeability can avoid interruption to the central nervous system[59]. P-glycoprotein (PGP) substrates are being actively effluxed from the cells thereby resulting in low absorption into the blood circulation[60,61]. Besides these, cytochrome P450 enzymes are crucial in the metabolism of most clinical drugs. Hence, the inhibition of cytochrome P450 enzymes can lead to decreased drug metabolism and possibly, adverse health complications, due to drug-drug interaction upon co-prescription with other drugs[62,63]. Moreover, the drug-likeness rules, such as the Lipinski rule of five, work by predicting pharmacological behavior upon oral administration based on the chemical properties of potential drugs[64]. Lastly, bioavailability takes consideration of both absorption and distribution of the drugs, of which the eventual presence in blood circulation upon oral consumption is evaluated.

DnaK protein belongs to the 70 kDa heat shock protein (HSP70) family, which functions as molecular chaperone mediated by its ATPase activities[65]. DnaK protein has been reported to be central in mediating bacterial stress responses. Among these, increase in antimicrobial susceptibilities and decrease in survivability in host, have been manifested in DnaK mutants[66–68]. Moreover, our previous work on whole-genome analysis (WGA) of protein interaction network (PIN) reported that DnaK protein was crucial in mediating quorum sensing in multidrug resistant *Proteus mirabilis*[69]. Furthermore, WGA analyses of PIN from MDR pathogens like *P. aeruginosa*, S. *aureus*, *S. enterica*, *S. pneumoniae*, *P. mirabilis*, *Acinetobacter baumannii*, *Escherichia coli* and *Mycobacterium tuberculosis* revealed DnaK to be among the top 10 crucial proteins indispensable for the cellular integrity of the bacteria[70]. Also, the ATP-binding pocket of DnaK chaperone has been indicated to be druggable and shown promise to cope with MDR in both gram negatives and positives (Tan & Lahiri, unpublished data). Hence, DnaK protein has been selected for the *in-silico* study, herein, as a promising drug target for MDR bacteria by inhibiting its ATP binding pocket, which can result in its impairment of chaperone function.

Through our computational screening of the chemical libraries of the *N. lappaceum L.* fruit epicarp extractions, Catechin (C), Eplerenone (E), and Oritin-4-beta-ol (O) were shortlisted as the promising antimicrobials in combating the MDR pathogens by dint of their capacity in targeting the DnaK protein and having good pharmacological profiles. Despite being PGP substrate, C has manifested strong binding affinity to DnaK and therefore, can result in effective DnaK functional inhibition with a small amount. Otherwise, PGP inhibitors like C can be co-prescribed easily as it has a good metabolic profile. Moreover, C has been well-characterized for its antibacterial activities and known for its ability to cause leakage of bacterial cellular contents along with increased intracellular reactive oxygen species production in both gram negatives and positives[71,72]. However, the biological targets of C have not been described. As DnaK protein is crucial in bacterial stress response, by inhibiting the DnaK chaperone function, the bacterial cellular and biomolecular integrity can be affected upon receiving environmental oxidative stress. Herein, we showed that in *P. aeruginosa*, C could bind stably to the ATP-binding pocket of DnaK throughout the MD simulation with 3 stable active residues (LYS 70, GLU 171, and GLU 267), while maintaining the ATP-bound conformation of the DnaK protein without the necessity for ATP binding (**Fig. 2B, 3A**). This reflected the inability of the ATP molecules to bind the CPaD (Catechin-bound DnaK protein of *P. aeruginosa*) as also a complete halting of the normal DnaK chaperone function via conformational changes ensuing ATP hydrolysis. However, C could not inhibit SaD (DnaK of *S. aureus*) the same way, due to its inability to maintain the integrity of NBD domain and thereby escaping from the binding pocket. It is this binding pocket which allows subsequent binding of ATP molecules on DnaK to continue the chaperone function. On the contrary, herein, we present the discovery of two novel potential compounds, E and O, whose antibacterial activities have not been reported and/or described earlier. Notably, E has been widely utilized in cardiovascular implications and as diuretics[73,48]. O, however, has not been explored to confer any biological significance. Despite that, it is notable that the chemical structure of O is analogous to C (**Fig. 1**), with the sites of hydroxylation being slightly different.

Throughout the molecular dynamics simulation (MDS) processes, only 1 or 2 hydrogen bonds can be observed in EPaD and ESaD, which suggested weak protein-ligand electrostatic interactions. This can be explained by the chemical structure of E, being crowded with carbonyls and ethers which are weak bases, and hydroxyl groups are lacking. The ligand, however, has been retained in the docking pocket over the course of MDS. This probably suggests that hydrophobic (van der Waals) interactions were dominant in this case. This was reflected through the intermolecular interaction energies (**Fig. 3F**), of which the Lennard-Jones potentials were much higher than Coulomb potentials in Eplerenone-DnaK (ED) complexes, while the reverse was observed in for C and O. Moreover, the binding conformation of E in PaD did not “cover up” completely at the binding site of phosphate groups of the ATP for which further wet-lab confirmation is required. Furthermore, among the three ligands simulated, O manifested the best binding capabilities to both PaD and SaD with rich intermolecular electrostatic interactions and highest total interaction energies. After MDS, the active residues THR 11 and ASP 194 were retained in OPaD, while GLY 312 was retained in OSaD. Again, despite being structurally analogous to C, O manifested good predicted pharmacological properties in all the aspects considered. Therefore, with better binding capabilities to DnaK receptor and pharmacological properties, herein we report O to be a more potent

antibacterial compound compared to the well-known C, which is active against both the gram positive and negative bacteria.

Conclusion

Our findings reinstate the promising antibacterial effects, of the yellow variety of Malaysian Rambutan *(N. lappaceum L.)* fruit epicarp crude extracts, against selected Gram-positive and Gram-negative MDR pathogens. In this context, particularly ethyl acetate and acetone (sequential and direct) extracts demonstrated remarkable antibacterial effects toward all tasted pathogens, while remaining fractions including, chloroform, ethanol, methanol and water did not exhibit such potential. Nevertheless, *N. lappaceum* presents itself to be a novel source for antibacterial compounds with high potential for the development of pharmaceutically valuable drugs. Further studies are mandatory to separate the specific compound(s) responsible for the desired effects, and to develop our knowledge on the other unseen potentials in *N. lappaceum.*

Materials And Methods

Solvents.

All solvents, used for preparation of crude extractions, were of HPLC grades In order of increasing polarities, these were Chloroform (99.9%, Sigma-Aldrich, LiChrosolv, Malaysia), Ethyl acetate, Acetone (99.5% Chemiz, Malaysia), Ethanol, Methanol (99.8%, ChemAR, Systerm, Malaysia) and double distilled Milli-Q Type 1 water (MilliporeMerck, Germany). Solvents used for LC-MS and GC-MS were of MS grades.

Plant Product.

The yellow variety fruits of *N. lappaceum L.* were purchased from local marketplace, Bandar Sunway, Selangor, Malaysia.

Tested microorganisms.

Six clinical isolates, used in the study, were obtained from the Department of Biological Sciences, Sunway University, Malaysia. These were *Streptococcus pyogenes* (ATCC-49399), *Bacillus subtilis* (ATCC-11774), methicillin-resistant *Staphylococcus aureus* (MRSA) (MTCC-381123), *Pseudomonas aeruginosa* (ATCC-10145), *Klebsiella pneumoniae* (ATCC-700603) and *Salmonella enterica* (ATCC-14028). All strains were tested to be multidrug resistant[74].

Preparation of crude extracts.

Epicarp crude extracts were prepared following the method of Do *et al.*[75] using the solvents mentioned earlier for the direct extracts. For the sequential method of extraction, the mentioned solvents were used in order of increasing polarity *viz* chloroform<ethyl acetate<acetone<ethanol<methanol<water. In both the cases, essentially, the peels of *N. lappaceum* were removed from the fruit and washed thoroughly with running, followed by, distilled water to remove contaminants and thereafter dried using freeze-dryer. Dried peels were ground into fine powder using an electric grinder. To produce different fractions of crude extracts, 10 g of powder was extracted in 100 mL of selected solvents. The solution was mixed thoroughly by using incubator shaker (Yihder LM-530D Incubator Shaker, Taiwan) for 24 h. To separate supernatant, the solution was centrifuged (Eppendorf 5810 R Centrifuge, Germany) at 4000 rpm for 10 min at 4 °C to completely eliminate the leftover fine sediments. The solvent extracts were concentrated using Rotary evaporator, and further with vacuum concentrator until a viscous extract was obtained. All extracts were stored at 4°C for future experiments.

Potential *in-vitro* antibacterial activities of yellow rambutan fruit epicarp extracts.

Disc Diffusion assay.

Seed culture of the tested pathogen was consistently swabbed on agar plate. Sterilized blank paper discs were separately impregnated by different concentration of extracts (250 to 2000µg/ml) and placed on agar plate. The plates were incubated at 37ºC for 16h. The antibacterial activity was noted by measuring the diameter of inhibition zone. Gentamicin (10µg/disc) was used as positive control while DMSO (<1%) was kept as negative control. All the experiments had technical triplicates and were performed twice to render two biological replicates.

Broth Dilution Assay.

A broth micro-dilution method was used to evaluate the minimum inhibitory concentration (MIC) values of crude extracts using Clinical & Laboratory Standards Institute (CLSI) procedures. Each extract (5µL) was added into the wells of a 96 well plate comprising 10^5 CFU/mL bacterial cells. The 96 well plates were incubated at 37°C for 16 h. Final concentrations ranged from 250 to 2000 µg/mL. Three controls comprising, gentamicin 10µg/mL (positive control), DMSO <1% (solvent control) and bacterial inoculum (negative control) were included in each test. The lowest concentration of the tested extract showing inhibitory effect against the pathogens, recorded via the Microplate reader (TECAN, Infinite-M200-PRO), was taken as the MIC value. All tests, having technical triplicates, were confirmed twice. Both the fractions of ethyl acetate and acetone extracts gave promising results with which all chromatographic analyses were carried out.

Exploration of chemical constituents through chromatographic analyses.

High performance Liquid Chromatography (HPLC).

Ethyl acetate and acetone extracts were used as samples for qualitative phytochemical screening via HPLC using Agilent-1260 infinity system, according to the reported method of Zeb[76]. Briefly, one-gram sample extract was mixed in methanol and water (1:1; 20 mL; v/v) and heated at 70˚C for 1 hour in water bath. This was centrifuged at 4000 rpm for 10 minutes and 2 mL of the supernatant was filtered into HPLC vials through Whatman filter paper. The separation was performed via Agilent-Zorbax-Eclipse column (XDB-C18). Column gradients system comprised solvent B and C. Solvent B consisted of deionized water: methanol: acetic acid having a ratio of 180: 100: 20; v/v while solvent C had deionized water: methanol: acetic acid in the ratio of 80: 900: 20; v/v. Gradient system was started by solvent B for 100%, 85%, 50% and 30% at 0, 5, 20 and 25 minutes followed by solvent C (100%) from 30-40 minutes. Elution occurred after 25 minutes. The ultraviolet array detector (UVAD) was set at 280 nm for the antioxidants analysis and chromatogram were documented using retention times. UV spectra of compounds and accessible standards along with quantification was carried out by taking the percent peak area. Quantification of the antioxidants was measured by formula:

$$Cx = \frac{Ax \times Cs\left(\mu g/_{ml}\right) \times V(ml)}{As \times Sample\ (wt.in\ g)} \qquad (1)$$

Cx= Sample concentration; *As*= Standard peak area; *Ax*= Sample peak area; *Cs*= Standard concentration (0.09 µg/ml).

Liquid Chromatography and Mass Spectrometry (LC-MS).

A mixture of standards and new metabolites found in the ethyl acetate and acetone fractions were analyzed via LC-MS exactly as per the method reported by Yap *et al.*[77]. In order to eradicate systematic errors, reference solution was used with the two ions, having m/z of 121.0508 and 92266.0097, being selected for mass calibration. Finally, the mass spectra for the compounds present in ethyl acetate (EA) and acetone (AC) fractions were run against the database of NIST (National Institutes of Standard and Technology, Gaithersburg, MD, USA) Mass Spectral Search Program-2009 version 2 for the documentation of homologous compounds over Agilent Mass-Hunter Qualitative Analysis B.05.00 software.

Gas chromatography–mass spectrometry (GC-MS).

Ethyl acetate and Acetone fractions were subjected to gas chromatography-mass spectrometry (GC-MS) analysis, using Agilent technologies model 7890B GC System coupled with Pegasus HT High Throughput TOFMS (Leco Corp., MI, USA). An aliquot of an extract of 1ml was injected to the GC-MS apparatus. Next, Agilent J&W HP-5MS (phenyl methyl siloxane, length 30 m, Dia. 0.32 mm, Film, 0.25µm) analytic column was used to separate components under an inert atmosphere of helium (1.5 mL/min). Other standardized parameters utilized during the process: oven temperature of 80°C (2 min) was increased to a temperature of 300°C at the rate of 3°C/min, solvent delay time was 5 min, inlet line temperature was 225°C, and ion source temperature was 250°C. Mass spectra were taken at 70 eV and acquisition mode-scan was 20-1000 amu while sixty-four (64) minutes was the GC run time. The interpretation of mass spectrum and documentation of phytochemicals present in the fractions were achieved via the database of NIST libraries.

Virtual Screening of Chemical determinants from chromatographic analyses.

In silico Protein Model Generation.

S. aureus (*Sa*) and *P. aeruginosa* (*Pa*) were chosen as gram-positive and gram-negative bacterial representatives for computational analyses of DnaK protein binding. 3D structures of DnaK proteins, from the aforesaid species, were generated via homology modelling using MODELLER version 9.24[78]. DnaK has two conformations, namely, the open or ATP-bound and the closed or ADP-bound conformation[65]. Herein, we focused on the open conformation of DnaK, to identify potential competitive inhibitors of ATP in order to prevent proper functioning of DnaK protein.

The protein sequences of *Sa* and *Pa* DnaK were obtained from UniProtKB with accession IDs of Q2FXZ2 and A6VCL8 (UniProt Consortium, 2019), respectively. To search for suitable homology modelling templates, both NCBI BLASTp and the MODELLER in-built build_profile.py were utilized[78,79]. For *Pa* DnaK (PaD), the templates were full-length ATP-bound *E. coli* (*Ec*) DnaK protein structures (PDB ID: 5NRO, Chain: A, Query Coverage (QC): 94%, Percent Identity (PI): 79.50%, Resolution (R): 3.25 Å; PDB ID: 4JNE, Chain: A, QC: 94%, PI: 78.80%, R: 1.96 Å; and PDB ID: 4B9Q, Chain: A, QC: 94%, PI: 77.96%, R: 2.40 Å). For *Sa* DnaK (SaD), besides the aforementioned *Ec* DnaK (EcD) models, one additional template, from *Geobacillus kaustophilus* DnaK protein (PDB ID: 2V7Y, Chain: A), was selected due to the high percentage of sequence identity expected as per the gram positive character of *S. aureus* and *G. kaustophilus*. As this template structure was in closed conformation and we were only interested in the open conformation, only the Nucleotide Binding Domain (NBD, residues 1 to 350 in template model) which does not differ much in both conformations, were taken into consideration for homology modelling, and the remaining C-terminal residues modelling were guided by the *Ec* models to shape an open conformation. Therefore, the

templates for SaD were (PDB ID: 2V7Y, Chain: A, Template Residues: 1-350, QC: 57%, PI: 83.19%, R: 2.37 Å; PDB ID: 5NRO, Chain: A, QC: 93%, PI: 56.19%, R: 3.25 Å; PDB ID: 4JNE, Chain: A, QC: 92%, PI: 55.54%, R: 1.96 Å; and PDB ID: 4B9Q, Chain: A, QC: 94%, PI: 55.43%, R: 2.40 Å). 5 homology models were generated for each protein of SaD and PaD, and the models with lowest DOPE (discrete optimized protein energy) scores were selected for downstream virtual screening for both. The SaD and PaD homology models were validated via Swiss-Model Structure Assessment and SAVES v5.0 servers[80] (Table S7).

Druggable Pocket Validation.

To validate the druggability of the ATP docking pocket, we have conducted ligand binding site prediction using P2Rank from PrankWeb server[81]. P2Rank predicts the chemical druggability on protein solvent-accessible surface via a non-templated machine learning approach. The ATP binding pocket was predicted to be druggable and ranked first in both cases of SaD and PaD (Table S8; Fig. S8). These pockets from SaD and PaD were further considered to be targeted for virtual screening.

Molecular Docking with Chemical Determinants.

POAP pipeline, Samdani & Vetrivel[82] was followed for an *in silico* virtual screening of the chemical compounds obtained through different chromatographic separation. SMILES notations of these compounds were obtained and their 3D models (in mol2 format) were generated through POAP Ligand Preparation pipeline. To this end, Chimera was utilized to generate physiological protonation states of ligands, and PDBQT files were prepared[83]. Ligand optimizations were carried out via POAP Ligand Preparation pipeline utilizing MMFF94 force field, being optimized for drug-like organic molecules and molecular docking[84]. Out of the 50 conformers, generated for each ligand through Weighted Rotor Search approach, only the best conformers were retained. Finally, the ligands were subjected to energy minimization for 5000 steps by the conjugate algorithm.

The macromolecule receptors, pertaining to the SaD and PaD proteins, were prepared using AutoDockTools. AutoDock 4.2, aided by POAP pipeline, was utilized for the virtual screening process[85]. For AutoDock parameters, 100 generations of Lamarckian Genetic Algorithm were set for each protein-ligand complex. To fit in the previously predicted pocket, docking grids were adjusted into squares of 24 Å with x, y, z coordinates of 17.647, 75.43, 27.766, and 18.069, 74.299, 28.532, for SaD and PaD, respectively. For the silicon-containing compound among the set of ligands, molecular docking was separately carried out with AD4.1_bound parameter file, obtained from AutoDock, wherein parameters for silicon atoms (Rii=4.3; eii=0.402) were added[86].

Pharmacological Properties Screening.

Pharmacological properties, encompassing pharmacokinetics, drug likeness, and molecular information for each chemical compound, were predicted using SwissADME[87].

Molecular Dynamics Simulation.

Ensuing virtual and pharmacological screenings, potential drug candidates were rationally selected to undergo molecular dynamics (MD) simulation via GROMACS version 2019.3[88]. CHARMM36 force field (Version July, 2020), along with TIP3P water model, was utilized for macromolecule processing[89]. Avogadro software was utilized for mol2 format conversion and complete protonation (protonation of non-polar atoms)[90]. The Perl script, sort_mol2_bonds.pl, written by Justin Lemkul was utilized for bond order arrangements in ligand mol2 files. Then, topologies of the ligand models were generated through CGenFF server, and a python script (cgenff_charmm2gmx.py) was utilized to convert topologies for CHARMM to GROMACS[91]. Solvation was carried out in a dodecahedron box ranged 1.0 Å from the protein-ligand complex. The system was then being ionized to achieve electrostatic neutralization. Subsequently, the system was subjected to energy minimization via steepest descent algorithm until convergence at maximum force of less than 1000 kJ mol^{-1} nm^{-1} (Fig. S9). Potential energy shifts of the systems were monitored herein.

Equilibration of the systems were carried out via NVT and NPT ensembles for 50000 steps (100ps), with temperature, pressure, and density shifts being monitored therein. Subsequently, production MD simulations were carried out for 5000000 steps (10ns) to observe protein-ligand interactions. RMSD (Root Mean Square Deviation) values of ligands and receptors, number of hydrogen bonds between ligands and receptors, and ligand-receptor interaction energies (Coulombic interaction energies and Lennard-Jones energies) were computed throughout the MD simulations. Total interaction energies were computed, and errors were estimated via error propagation by addition.

Declarations

Acknowledgments

The authors wish to acknowledge Sunway University, Selangor, Malaysia for the provision of necessary computational facilities. We thank Pang Jun Rui, Noor Akbar, Liew Tuck Onn and Rohit Mishra for providing, assistance of varying kinds, in different parts of the project.

Author contributions

CL conceived the concepts, planned and designed the analyses. AA extracted the natural products and assessed their antibacterial activities. MZ conducted and analyzed HPLC, helped by AA. SA conducted LC-MS with the results being analyzed by AA and CL. YYY provided the plant products and co-supervisory

inputs along with EK. YCT conducted the computational part with occasional inputs from CL. Concepts for artwork were generated and executed by AA and TCY with guidance provided by CL. AA and YCT primarily wrote the manuscript aided by editorial upgradation by CL.

Additional Information

The authors declare that they have no conflict of interest, financial or otherwise, for this reasearch.

References

1. Maheshwari, Meenu, Iqbal Ahmad, and Abdullah Safar Althubiani. "Multidrug resistance and transferability of blaCTX-M among extended-spectrum β-lactamase-producing enteric bacteria in biofilm." Journal of Global Antimicrobial Resistance 6 (2016): 142-149.
2. Dockrill, P. (2017) The 12 deadliest drug-resistant bacteria have officially been ranked. Science Alert. (https://www.sciencealert.com/the-12-deadliest-drug-resistant-bacteria-have-officially-been-ranked).
3. Obeng-Nkrumah, Noah, et al. "High levels of extended-spectrum beta-lactamases in a major teaching hospital in Ghana: the need for regular monitoring and evaluation of antibiotic resistance." The American journal of tropical medicine and hygiene 89.5 (2013): 960-964.
4. Barbieri, Ramona, et al. "Phytochemicals for human disease: An update on plant-derived compounds antibacterial activity." Microbiological research 196 (2017): 44-68.
5. Cheesman, Matthew J., et al. "Developing new antimicrobial therapies: are synergistic combinations of plant extracts/compounds with conventional antibiotics the solution?." Pharmacognosy reviews 11.22 (2017): 57.
6. Djeussi, Doriane E., et al. "Antibacterial activities of selected edible plants extracts against multidrug-resistant Gram-negative bacteria." BMC complementary and alternative medicine 13.1 (2013): 164.
7. Mandalari, G., et al. "Antimicrobial activity of flavonoids extracted from bergamot (Citrus bergamia Risso) peel, a byproduct of the essential oil industry." Journal of applied microbiology 103.6 (2007): 2056-2064.
8. Katalinić, Višnja, et al. "Polyphenolic profile, antioxidant properties and antimicrobial activity of grape skin extracts of 14 Vitis vinifera varieties grown in Dalmatia (Croatia)." Food chemistry 119.2 (2010): 715-723.
9. Vattem, D. A., et al. "Antimicrobial activity against select food-borne pathogens by phenolic antioxidants enriched in cranberry pomace by solid-state bioprocessing using the food grade fungus Rhizopus oligosporus." Process Biochemistry 39.12 (2004): 1939-1946.
10. Kanatt, Sweetie R., Ramesh Chander, and Arun Sharma. "Antioxidant and antimicrobial activity of pomegranate peel extract improves the shelf life of chicken products." International journal of food science & technology 45.2 (2010): 216-222.

11. Oliveira, Daniela A., et al. "Nanoencapsulation of passion fruit by-products extracts for enhanced antimicrobial activity." Food and Bioproducts Processing 104 (2017): 137-146.
12. Nguyen, Nhat Minh Phuong, et al. "In vitro antioxidant activity and phenolic profiles of tropical fruit by-products." International Journal of Food Science & Technology 54.4 (2019): 1169-1178.
13. Zhuang, Yongliang, et al. "Protective effects of rambutan (Nephelium lappaceum) peel phenolics on H2O2-induced oxidative damages in HepG2 cells and d-galactose-induced aging mice." Food and Chemical Toxicology 108 (2017): 554-562.
14. Suhendi, Andi. "Potential Activity of Rambutan (Nepheliumlappaceum L.) Fruit Peel Extract as Antidiabetic and Antihypercholesterolemia." (2015).
15. Malini, C. "Mahesh kumar R. Evaluation of bioactive potential in rambutan fruit (Nephelium lappaceum) samplesusing pathogens." Global J. Engg. Appl. Sci 3.3 (2013): 138-142.
16. Bhat, Ramesa Shafi, and Sooad Al-daihan. "Antimicrobial activity of Litchi chinensis and Nephelium lappaceum aqueous seed extracts against some pathogenic bacterial strains." Journal of King Saud University-Science 26.1 (2014): 79-82.
17. Thitilertdecha, Nont, Aphiwat Teerawutgulrag, and Nuansri Rakariyatham. "Antioxidant and antibacterial activities of Nephelium lappaceum L. extracts." LWT-Food Science and Technology 41.10 (2008): 2029-2035.
18. Sekar, Mahendran, et al. "Comparative evaluation of antimicrobial properties of red and yellow rambutan fruit peel extracts." Annual Research & Review in Biology (2014): 3869-3874.
19. Padmavathi, Alwar Ramanujam, Bose Abinaya, and Shunmugiah Karutha Pandian. "Phenol, 2, 4-bis (1, 1-dimethylethyl) of marine bacterial origin inhibits quorum sensing mediated biofilm formation in the uropathogen Serratia marcescens." Biofouling 30.9 (2014): 1111-1122.
20. Gul, Parveen, and Jehan Bakht. "Antimicrobial activity of turmeric extract and its potential use in food industry." Journal of food science and technology 52.4 (2015): 2272-2279.
21. Lee, Hoi-Seon. "Antimicrobial properties of turmeric (Curcuma longa L.) rhizome-derived ar-turmerone and curcumin." Food Science and Biotechnology 15.4 (2006): 559-563.
22. Yusuf, Amina J., et al. "Antimicrobial activity of stigmasterol from the stem bark of Neocarya macrophylla." Journal of Medicinal Plants for Economic Development 2.1 (2018): 1-5.
23. de Dieu Tamokou, Jean, et al. "Antioxidant and antimicrobial activities of ethyl acetate extract, fractions and compounds from stem bark of Albizia adianthifolia (Mimosoideae)." BMC Complementary and Alternative Medicine 12.1 (2012): 99.
24. Tintino, Saulo R., et al. "Action of cholecalciferol and alpha-tocopherol on Staphylococcus aureus efflux pumps." EXCLI journal 15 (2016): 315.
25. Lipinski, Christopher A. "Lead-and drug-like compounds: the rule-of-five revolution." Drug Discovery Today: Technologies 1.4 (2004): 337-341.
26. Ghose, Arup K., Vellarkad N. Viswanadhan, and John J. Wendoloski. "A knowledge-based approach in designing combinatorial or medicinal chemistry libraries for drug discovery. 1. A qualitative and

quantitative characterization of known drug databases." Journal of combinatorial chemistry 1.1 (1999): 55-68.

27. Veber, Daniel F., et al. "Molecular properties that influence the oral bioavailability of drug candidates." Journal of medicinal chemistry 45.12 (2002): 2615-2623.
28. Egan, William J., Kenneth M. Merz, and John J. Baldwin. "Prediction of drug absorption using multivariate statistics." Journal of medicinal chemistry 43.21 (2000): 3867-3877.
29. Muegge, Ingo, Sarah L. Heald, and David Brittelli. "Simple selection criteria for drug-like chemical matter." Journal of medicinal chemistry 44.12 (2001): 1841-1846.
30. Hann, Michael M., and György M. Keserü. "Finding the sweet spot: the role of nature and nurture in medicinal chemistry." Nature reviews Drug discovery 11.5 (2012): 355-365.
31. Abdella, Mohamed, Bahaa Abdella, and Chandrajit Lahiri. "Rediscovering and repurposing natural microbial macromolecules through computational approaches." Microbial and Natural Macromolecules. Academic Press, 2020. 373-400
32. Bakari, Sana, et al. "Proximate analysis, mineral composition, phytochemical contents, antioxidant and antimicrobial activities and GC-MS investigation of various solvent extracts of cactus cladode." Food Science and Technology 37.2 (2017): 286-293.
33. Mohamed, Suhaila, Zaharia Hassan, and Norhasimah Abdul Hamid. "Antimicrobial activity of some tropical fruit wastes (guava, starfruit, banana, papaya, passionfruit, langsat, duku, rambutan and rambai)." Pertanika 17 (1994): 219-219.
34. Thitilertdecha, Nont, et al. "Identification of major phenolic compounds from Nephelium lappaceum L. and their antioxidant activities." Molecules 15.3 (2010): 1453-1465.
35. Tadtong, Sarin, et al. "Antibacterial activities of rambutan peel extract." Journal of Health Research 25.1 (2011): 35-37.
36. Nazir, Nausheen, et al. "Phytochemical analysis, molecular docking and antiamnesic effects of methanolic extract of Silybum marianum (L.) Gaertn seeds in scopolamine induced memory impairment in mice." Journal of ethnopharmacology 210 (2018): 198-208.
37. Nazir, Nausheen, et al. "Phytochemical analysis and antidiabetic potential of Elaeagnus umbellata (Thunb.) in streptozotocin-induced diabetic rats: pharmacological and computational approach." BMC complementary and alternative medicine 18.1 (2018): 332.
38. Song, Fei, et al. "Antibacterial effect of fosfomycin tromethamine on the bacteria inside urinary infection stones." International Urology and Nephrology (2019): 1-10.
39. Adamczak, A., Ożarowski, M. and Karpiński, T.M., 2020. Antibacterial activity of some flavonoids and organic acids widely distributed in plants. Journal of Clinical Medicine, 9(1), p.109.
40. Karuppiah, Vijayakumar, and Ramanathan Thirunanasambandham. "Quebrachitol from Rhizophora mucronata inhibits biofilm formation and virulence production in Staphylococcus epidermidis by impairment of initial attachment and intercellular adhesion." Archives of Microbiology (2020): 1-14.

41. Metwally, A. M., et al. "Phytochemical investigation and antimicrobial activity of Psidium guajava L. leaves." Pharmacognosy magazine 6.23 (2010): 212.
42. Sledz, Wojciech, et al. "Antibacterial activity of caffeine against plant pathogenic bacteria." Acta Biochimica Polonica 62.3 (2015).
43. Yi, H.S., Ahn, Y.R., Song, G.C., Ghim, S.Y., Lee, S., Lee, G. and Ryu, C.M., 2016. Impact of a bacterial volatile 2, 3-butanediol on Bacillus subtilis rhizosphere robustness. Frontiers in Microbiology, 7, p.993.
44. De, Ronita, et al. "Antimicrobial activity of ellagic acid against Helicobacter pylori isolates from India and during infections in mice." Journal of Antimicrobial Chemotherapy 73.6 (2018): 1595-1603.
45. Başpınar, Yücel, Mustafa Kotmakçı, and Ismail Öztürk. "Antimicrobial Activity of Phytosphingosine Nanoemulsions against Bacteria and Yeasts." Celal Bayar Üniversitesi Fen Bilimleri Dergisi 14.2 (2018): 223-228.
46. Kotsiou, A., et al. "Impact of experimental trauma and niflumic acid administration on antimicrobials' concentration in serum and mandible of rats." JOURNAL OF MUSCULOSKELETAL AND NEURONAL INTERACTIONS 6.3 (2006): 242.
47. Pham, Thu Ha, et al. "An update on the effects of glyceollins on human health: possible anticancer effects and underlying mechanisms." Nutrients 11.1 (2019): 79.
48. Pierson-Marchandise, Marion, et al. "The drugs that mostly frequently induce acute kidney injury: a case– noncase study of a pharmacovigilance database." British Journal of Clinical Pharmacology 83.6 (2017): 1341-1349.
49. da Silva Sa, Fabyola Amaral, et al. "Phytochemical analysis and antimicrobial activity of Myrcia tomentosa (Aubl.) DC. Leaves." Molecules 22.7 (2017): 1100.
50. Heliawati, Leny, Yana Maolana Syah, and Miranti Banyuning Bumi. "Bryononic Acid: Antibacterial Compound from Fruit Hulls of S. koetjape Merr Extract."
51. Prieto Rodríguez, Juliet Angélica, et al. "Estudio fitoquímico de hojas de Uncaria guianensis y evaluación de actividad antibacteriana." Acta amaz (2011): 303-310.
52. Bylka, W., I. Matlawska, and N. A. Pilewski. "Natural flavonoids as antimicrobial agents." Jana 7.2 (2004): 24-31.
53. Saradha Jyothi, K., and B. Subba Rao. "SCREE IG OF A TIBACTERIAL ACTIVITY OF EMBLICA OFFICI ALIS L. FRUITS."
54. Al-Harbi, Reham, et al. "Antibacterial and anti-hemolytic activity of tannins from Pimenta dioica against methicillin resistant Staphylococcus aureus." Bangladesh Journal of Pharmacology 12.1 (2017): 63-68.
55. Vu, Thuy Thu, et al. "Antibacterial activity of tannins isolated from Sapium baccatum extract and use for control of tomato bacterial wilt." PloS one 12.7 (2017): e0181499.
56. Sonfack, Gaiëlle, et al. "Saponin with antibacterial activity from the roots of Albizia adianthifolia." Natural Product Research (2019): 1-9.

57. Phuong, Nguyen Nhat Minh, et al. "Evaluation of antimicrobial activity of rambutan (Nephelium lappaceum L.) peel extracts." International Journal of Food Microbiology 321 (2020): 108539.
58. Hinds, L., et al. "Evaluating the antibacterial properties of polyacetylene and glucosinolate compounds with further identification of their presence within various carrot (Daucus carota) and Broccoli (Brassica oleracea) cultivars using high-performance liquid chromatography with a diode array detector and ultra-performance liquid chromatography–tandem mass spectrometry analyses." Journal of agricultural and food chemistry 65.33 (2017): 7186-7191.
59. Löbenberg, Raimar, et al. "Mechanism of gastrointestinal drug absorption and application in therapeutic drug delivery." Future Science Ltd, 2013. 8-22.
60. Amin, Md Lutful. "P-glycoprotein inhibition for optimal drug delivery." Drug target insights 7 (2013): DTI-S12519.
61. Prachayasittikul, Veda, and Virapong Prachayasittikul. "P-glycoprotein transporter in drug development." EXCLI journal 15 (2016): 113.
62. Gong, Yuqing, et al. "Pharmacokinetics and pharmacodynamics of cytochrome P450 inhibitors for HIV treatment." Expert opinion on drug metabolism & toxicology 15.5 (2019): 417-427.
63. Granfors, Marika T., et al. "Differential inhibition of cytochrome P450 3A4, 3A5 and 3A7 by five human immunodeficiency virus (HIV) protease inhibitors in vitro." Basic & clinical pharmacology & toxicology 98.1 (2006): 79-85.
64. Lipinski, Christopher A. "Lead-and drug-like compounds: the rule-of-five revolution." Drug Discovery Today: Technologies 1.4 (2004): 337-341.
65. Chiappori, Federica, et al. "DnaK as antibiotic target: hot spot residues analysis for differential inhibition of the bacterial protein in comparison with the human HSP70." PLoS One 10.4 (2015): e0124563.
66. Singh, Vineet K., et al. "Role for dnaK locus in tolerance of multiple stresses in Staphylococcus aureus." Microbiology 153.9 (2007): 3162-3173.
67. Yamaguchi, Yuko, et al. "Effects of disruption of heat shock genes on susceptibility of Escherichia coli to fluoroquinolones." BMC microbiology 3.1 (2003): 1-8.
68. Wolska, Krystyna I., et al. "Antibiotic susceptibility of Escherichia coli dnaK and dnaJ mutants." Microbial Drug Resistance 6.2 (2000): 119-126.
69. Pawar, Shrikant, et al. "In silico identification of the indispensable quorum sensing proteins of multidrug resistant Proteus mirabilis." Frontiers in cellular and infection microbiology 8 (2018): 269.
70. Mujawar, Shama, Amr Adel Ahmed Abd El-Aal, and Chandrajit Lahiri. "Variant Analysis from Bacterial Isolates Affirms DnaK Crucial for Multidrug Resistance." International Work-Conference on Bioinformatics and Biomedical Engineering. Springer, Cham, 2020.
71. Ajiboye, T. O., et al. "Contribution of reactive oxygen species to (+)-catechin-mediated bacterial lethality." Chemico-Biological Interactions 258 (2016): 276-287.

72. Sinsinwar, Simran, and Vellingiri Vadivel. "Catechin isolated from cashew nut shell exhibits antibacterial activity against clinical isolates of MRSA through ROS-mediated oxidative stress." Applied Microbiology and Biotechnology 104.19 (2020): 8279-8297.
73. Montalescot, Gilles, et al. "Early eplerenone treatment in patients with acute ST-elevation myocardial infarction without heart failure: The Randomized Double-Blind Reminder Study." European heart journal 35.34 (2014): 2295-2302.
74. Ali, Salwa Mansur, et al. "Biologically active metabolite (s) from haemolymph of red-headed centipede Scolopendra subspinipes possess broad spectrum antibacterial activity." AMB Express 9.1 (2019): 95.
75. Do, Quy Diem, et al. "Effect of extraction solvent on total phenol content, total flavonoid content, and antioxidant activity of Limnophila aromatica." Journal of food and drug analysis 22.3 (2014): 296-302.
76. Zeb, Alam. "A reversed phase HPLC-DAD method for the determination of phenolic compounds in plant leaves." Analytical Methods 7.18 (2015): 7753-7757.
77. Yap, Wing-Fai, et al. "Decoding Antioxidant and Antibacterial Potentials of Malaysian Green Seaweeds: Caulerpa racemosa and Caulerpa lentillifera." Antibiotics 8.3 (2019): 152.
78. Webb, Benjamin, and Andrej Sali. "Comparative protein structure modeling using MODELLER." Current protocols in bioinformatics 54.1 (2016): 5-6.
79. Altschul, Stephen F., et al. "Gapped BLAST and PSI-BLAST: a new generation of protein database search programs." Nucleic acids research 25.17 (1997): 3389-3402.
80. Waterhouse, Andrew, et al. "SWISS-MODEL: homology modelling of protein structures and complexes." Nucleic acids research 46.W1 (2018): W296-W303.
81. Jendele, Lukas, et al. "PrankWeb: a web server for ligand binding site prediction and visualization." Nucleic acids research 47.W1 (2019): W345-W349.
82. Samdani, A., and Umashankar Vetrivel. "POAP: A GNU parallel based multithreaded pipeline of open babel and AutoDock suite for boosted high throughput virtual screening." Computational biology and chemistry 74 (2018): 39-48.
83. Pettersen, Eric F., et al. "UCSF Chimera—a visualization system for exploratory research and analysis." Journal of computational chemistry 25.13 (2004): 1605-1612.
84. Halgren, Thomas A. "MMFF VI. MMFF94s option for energy minimization studies." Journal of Computational Chemistry 20.7 (1999): 720-729.
85. Morris, Garrett M., et al. "AutoDock4 and AutoDockTools4: Automated docking with selective receptor flexibility." Journal of computational chemistry 30.16 (2009): 2785-2791.
86. Saito, Hiroki, et al. "Phosphine boranes as less hydrophobic building blocks than alkanes and silanes: Structure-property relationship and estrogen-receptor-modulating potency of 4-phosphinophenol derivatives." Bioorganic & Medicinal Chemistry 28.4 (2020): 115310.

87. Daina, Antoine, Olivier Michielin, and Vincent Zoete. "SwissADME: a free web tool to evaluate pharmacokinetics, drug-likeness and medicinal chemistry friendliness of small molecules." Scientific reports 7 (2017): 42717.
88. Abraham, Mark James, et al. "GROMACS: High performance molecular simulations through multi-level parallelism from laptops to supercomputers." SoftwareX 1 (2015): 19-25.
89. Gutiérrez, Ignacio Soteras, et al. "Parametrization of halogen bonds in the CHARMM general force field: Improved treatment of ligand–protein interactions." Bioorganic & medicinal chemistry 24.20 (2016): 4812-4825.
90. Hanwell, Marcus D., et al. "Avogadro: an advanced semantic chemical editor, visualization, and analysis platform." Journal of cheminformatics 4.1 (2012): 17.
91. Vanommeslaeghe, Kenno, et al. "Automation of the CHARMM general force field for drug-like molecules." Biophysical Journal 100.3 (2011): 611a.

Figures

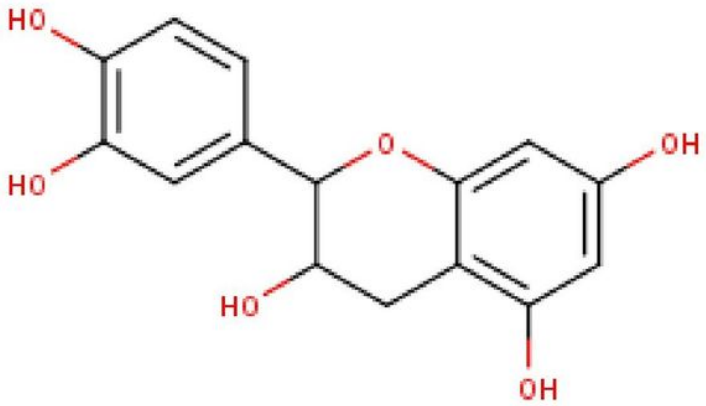

Catechin

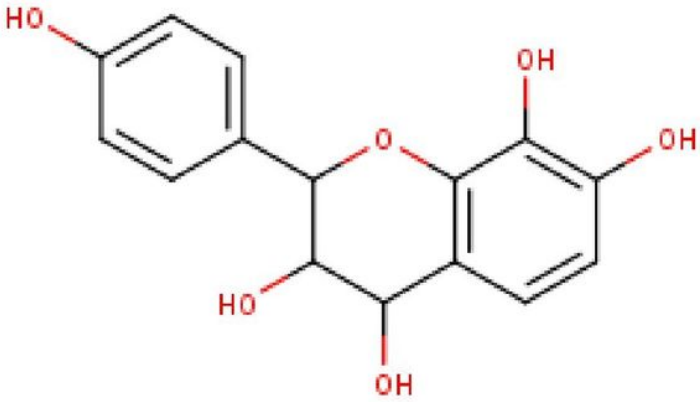

Oritin-4-beta-ol

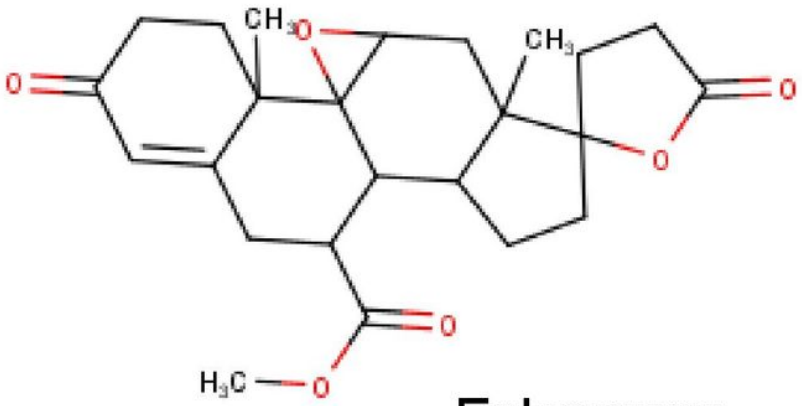

Eplerenone

Figure 1

Chemical Structure of Catechin, Oritin-4-beta-ol, and Eplerenone.

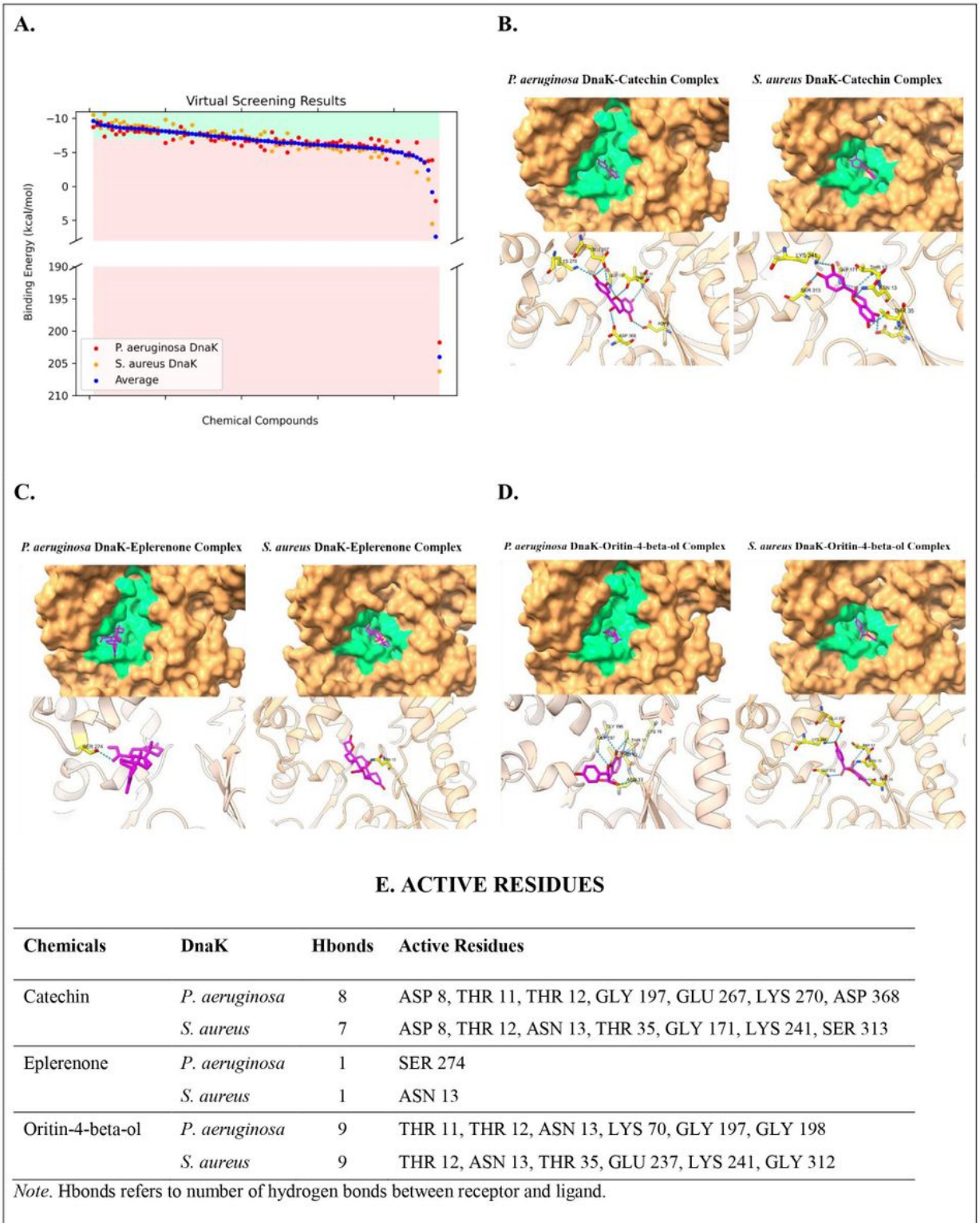

E. ACTIVE RESIDUES

Chemicals	DnaK	Hbonds	Active Residues
Catechin	*P. aeruginosa*	8	ASP 8, THR 11, THR 12, GLY 197, GLU 267, LYS 270, ASP 368
	S. aureus	7	ASP 8, THR 12, ASN 13, THR 35, GLY 171, LYS 241, SER 313
Eplerenone	*P. aeruginosa*	1	SER 274
	S. aureus	1	ASN 13
Oritin-4-beta-ol	*P. aeruginosa*	9	THR 11, THR 12, ASN 13, LYS 70, GLY 197, GLY 198
	S. aureus	9	THR 12, ASN 13, THR 35, GLU 237, LYS 241, GLY 312

Note. Hbonds refers to number of hydrogen bonds between receptor and ligand.

Figure 2

Results of virtual screening targeting P. aeruginosa and S. aureus DnaK proteins. A. Distribution of binding energies were plotted against screened compounds. Top binders with good pharmacological

properties, which are B. Catechin, C. Eplerenone, and D. Oritin-4-beta-ol were selected for analyses. P2Rank predicted binding pockets were coloured in green for visualization of ligands (magenta) binding to the receptor DnaK proteins (brown), with active sites (yellow) labelled. E. Intermolecular hydrogen bonds were tabulated with active residues listed.

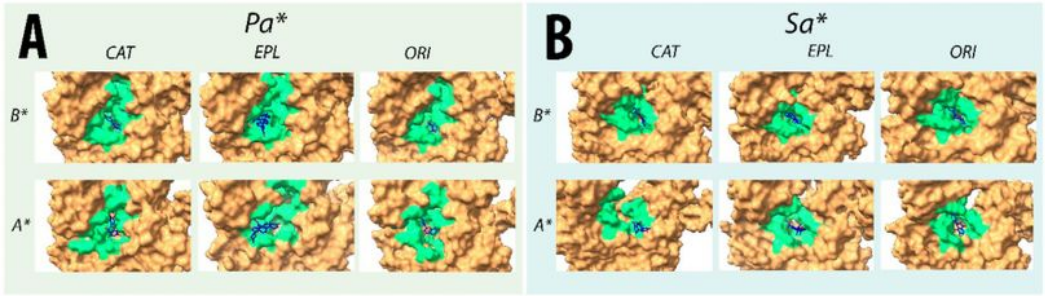

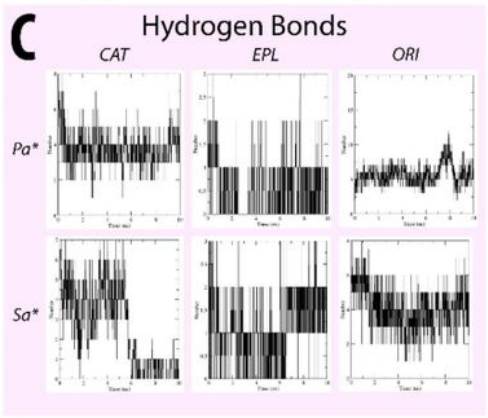

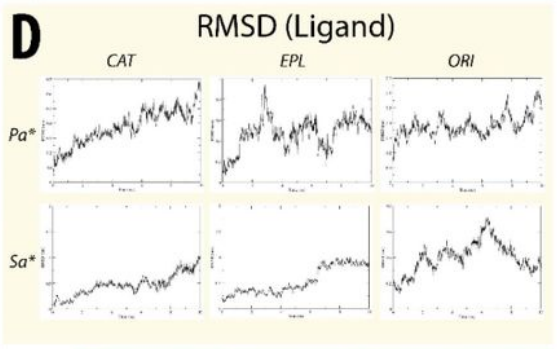

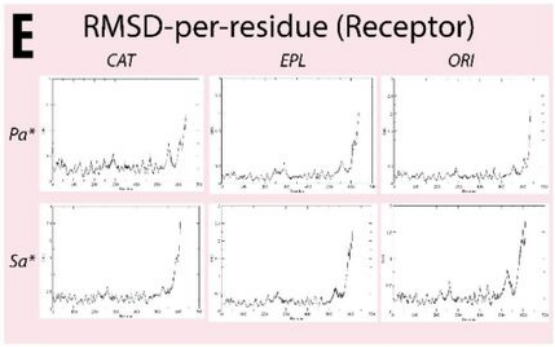

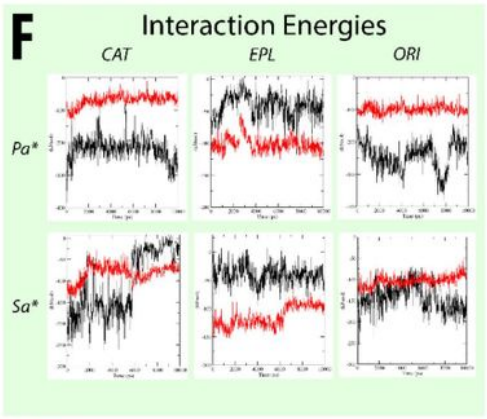

G

Active Residues

Ligand	Bacteria		Hbonds	Active Residues
CAT	Pa*	Before MD	7	ASP 8, **LYS 70**, **GLU 171**, GLY 197, **GLU 267**, ASP 368
		After MD	5	**LYS 70**, **GLU 171**, ASP 194, **GLU 267**
	Sa*	Before MD	6	ASP 8, GLY 10, THR 12, ASN 13, THR 35, SER 313
		After MD	1	CYS 15
EPL	Pa*	Before MD	1	**ARG 345**
		After MD	1	**ARG 345**
	Sa*	Before MD	2	ASN 13, LYS 240
		After MD	1	THR 12
ORI	Pa*	Before MD	6	**THR 11**, LYS 70, GLU 171, **ASP 194**, GLY 197, GLY 198
		After MD	9	**THR 11**, THR 12, **ASP 194**, LEU 195, ASP 233, GLN 343, THR 344
	Sa*	Before MD	5	THR 12, ASN 13, **GLY 312**, GLU 237, ASP 338
		After MD	2	**GLY 312**, GLU 339

Note. Hbonds refers to number of hydrogen bonds between receptor and ligand. Before MD refers to systems that went through energy minimization and NVE/NPT equilibration.

H

Interaction Enegies

Ligand	Bacteria	Interaction Energies	Average (kJ/mol)
CAT	Pa*	Coulomb	-219.9200 ± 8.2
		Lennard-Jones	-70.9474 ± 5.8
		Total	**-290.8674 ± 10.0**
	Sa*	Coulomb	-107.1020 ± 32.0
		Lennard-Jones	-82.0733 ± 6.6
		Total	**-189.1753 ± 32.7**
EPL	Pa*	Coulomb	-41.2606 ± 3.6
		Lennard-Jones	-101.537 ± 2.1
		Total	**-142.7976 ± 4.2**
	Sa*	Coulomb	-40.1841 ± 1.5
		Lennard-Jones	-114.11 ± 7.5
		Total	**-154.2491 ± 7.6**
ORI	Pa*	Coulomb	-244.537 ± 10
		Lennard-Jones	-99.0065 ± 1.5
		Total	**-343.5435 ± 10.1**
	Sa*	Coulomb	-143.712 ± 8.6
		Lennard-Jones	-103.7 ± 3.5
		Total	**-247.412 ± 9.3**

Note. Total interaction energies were calculated by the summation of Coulomb and Lennard-Jones interaction energies, with propagation of error estimation

Figure 3

MD simulation of A. P. aeruginosa and B. S. aureus DnaK (brown)-Catechin(blue) complexes, of which P2Rank predicted druggable pocket residues were colored in green for better visualization. C. Number of hydrogen bonds between receptor and ligand, D. RMSD values of Catechin, E. RMS fluctuation-per-residue of receptor macromolecule, and F. receptor-ligand interaction energies (Black: Coulombic interaction energies, Red: Lennard-Jones energies) were computed over the course of MD. G. Tabulated changes in number of hydrogen bonds and active residues before and after MD. H. Tabulated interaction energy values of DnaK-Catechin complexes Note. B* - Before MD, A* - After MD, Pa* - P. aeruginosa, Sa* - S. aureus, CAT – Catechin, EPL – Eplerenone, ORI – Oritin-4-beta-ol.

Supplementary Files

This is a list of supplementary files associated with this preprint. Click to download.

- SupplememtarydataofNLMSFinal.docx